

**Field- and angular-dependent resistance of  $\lambda$ -(BETS) $_2$ FeCl $_4$  under pressure**Y. J. Jo,\* Haeyong Kang,<sup>†</sup> and W. Kang<sup>‡</sup>*Department of Physics, Ewha University, Seoul 120-750, Korea*

S. Uji and T. Terashima

*National Institute for Material Science, Tsukuba, Ibaraki 305-0003, Japan*

T. Tanaka and M. Tokumoto

*National Institute of Advanced Industrial Science and Technology, Tsukuba, Ibaraki 305-8568, Japan  
and JST-CREST, Kawaguchi, Japan*

A. Kobayashi

*Graduate School of Science, The University of Tokyo, Bunkyo-ku, Tokyo 113-0033, Japan*

H. Kobayashi

*Institute for Molecular Science, Okazaki, Aichi 444-8585, Japan*

(Received 22 November 2005; revised manuscript received 7 March 2006; published 30 June 2006)

We measured the field strength and angular dependence in the electrical resistance of the organic conductor  $\lambda$ -(BETS) $_2$ FeCl $_4$  under a pressure of 6 kbar. In addition to the slow Shubnikov–de Haas (SdH) oscillations similar to those observed at ambient pressure, much faster oscillations are detected and attributed to the magnetic breakdown (MB) orbit. The increase of the SdH frequency indicates an increase in the size of the closed Fermi surface under pressure. The effective masses as determined from the closed and MB orbit oscillations are  $(2.9 \pm 0.3)m_0$  and  $(5.5 \pm 0.3)m_0$ , respectively. The effective mass becomes smaller under pressure most likely due to the broadening of the bandwidth. The estimated internal field increases from 32 to 52 T under a pressure of 6 kbar. Angular-dependent magnetoresistance oscillations reveal a very small closed orbit which is not detected in the SdH oscillation measurements.

DOI: [10.1103/PhysRevB.73.214532](https://doi.org/10.1103/PhysRevB.73.214532)

PACS number(s): 74.70.Kn, 74.25.Dw, 74.25.Ha, 74.62.Fj

**I. INTRODUCTION**

The band structure of organic molecular solids is mainly determined by the overlap of the molecular orbitals of the constituent molecules. The charge transfer salts based on the BETS [where BETS stands for bis(ethylenedithio)tetraselenafulvalene] molecule have Fermi surfaces (FS's) consisting of quasi-two-dimensional (quasi-2D) cylindrical pockets and extended corrugated planes.<sup>1,2</sup> Among various quasi-two-dimensional charge-transfer salts, the study of BETS compounds containing Fe<sup>3+</sup> magnetic ions has been of particular interest because the large magnetic moments of Fe<sup>3+</sup> ions would induce the  $\pi$ -electron spins on donor molecules to develop a  $\pi$ - $d$  coupled antiferromagnetic (AF) spin structure. Therefore, competition between the AF and superconducting (SC) states is expected. Electrical resistivity and magnetic susceptibility measurements reveal that the  $\pi$  conduction electrons from BETS molecules and the localized magnetic moments of the anions coexist down to very low temperature.

In general, the  $\pi$ - $d$  interaction destabilizes the superconductivity because the internal field by the magnetic ions has a tendency to destroy the Cooper pairs through the Zeeman effect. Surprisingly, superconductivity was discovered to be stabilized under high magnetic fields in  $\lambda$ -(BETS) $_2$ FeCl $_4$ . When a magnetic field is applied parallel to the conducting layer, the antiferromagnetically ordered Fe<sup>3+</sup> spins tend to align along the magnetic field, and a paramagnetic (PM) metallic state is induced at 10 T and the field-induced supercon-

ducting (FISC) state occurs between 18 and 41 T.<sup>3,4</sup> The appearance of the FISC state can be interpreted in terms of the Jaccarino-Peter compensation effect which states that the internal magnetic field  $H_{\text{int}}$  due to the aligned Fe<sup>3+</sup> ions compensates the external magnetic field.<sup>5</sup> Measurement of the SdH oscillations at ambient pressure revealed that there are oscillations with two distinct frequencies of 609 and 737 T. These frequencies correspond, respectively, to 14% and 17% of the first Brillouin zone (FBZ) estimated from the band calculation and their mean value agrees well with the area of the calculated FS.<sup>6</sup> The splitting of the Shubnikov–de Haas (SdH) oscillations is attributed to the spin-dependent FS separation due to the internal magnetic field. The strength of the internal field is related with the difference of two frequencies ( $F_1 - F_2 = 2\Delta F$ ) through the spin-splitting factor of the Lifshitz-Kosevich (LK) formula as follows:<sup>7,8</sup>

$$\Delta F = \frac{1}{4} g \frac{m_{\text{eff}}}{m_0} H_{\text{int}}. \quad (1)$$

For  $\lambda$ -(BETS) $_2$ FeCl $_4$  at the ambient pressure, the internal field is 32 T using  $m_{\text{eff}} = 4.1m_0$ .<sup>9</sup>

It is well known that applying high pressure is remarkably useful to the study of the electronic structure of organic metals, but only a few studies on  $\lambda$ -(BETS) $_2$ FeCl $_4$  have been performed under pressure. Magnetic susceptibility measurements under pressure suggested that the temperature of the AF metal-insulating transition decreases and the  $\pi$ - $d$  cou-

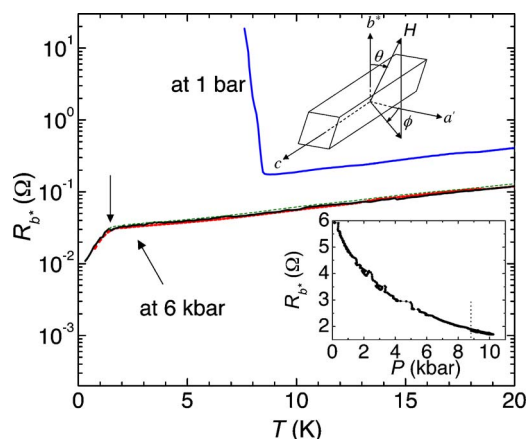


FIG. 1. (Color online) Temperature dependence of resistances of  $\lambda$ -(BETS) $_2$ FeCl $_4$  under a pressure values of 6 kbar. Three curves from experiments in the 18 T (black solid line), 33 T (red thick dashed line), and 14 T (green thin dashed line) magnets are superposed well one on another, representing a good stability of the sample and pressure. The trace of resistance at 1 bar (blue solid line) is also plotted for comparison. The kink around 1.3 K indicated by an arrow suggests that the AF order of the Fe $^{3+}$  spins occurs at this temperature. The lower right inset shows continuously decreasing resistance during application of the pressure at room temperature.

pling is reduced by pressure. Then, the AF order of Fe $^{3+}$  spins and the metallic  $\pi$  conduction electrons will coexist in  $\lambda$ -(BETS) $_2$ FeCl $_4$  at high pressure and the AF metallic state is stabilized. Finally, a SC state stabilizes at low temperature.<sup>10–12</sup> Balicas *et al.* reported the effect of a small pressure of 1.4 kbar on the magnetic-field–temperature phase diagram.<sup>13</sup> At 1.4 kbar, the SC state is stabilized at 5.6 K followed by an unusual SC to AF insulating transition at 4 K. Under a magnetic field, the field and temperature ranges of the FISC state broaden and the internal field slightly decreases.

With the purpose of achieving a better understanding of the  $\pi$ - $d$  interaction and the change of electronic properties under high pressure, we have measured the SdH oscillations and the angular-dependent magnetoresistance (AMR) of  $\lambda$ -(BETS) $_2$ FeCl $_4$  at a pressure of 6 kbar. Our experimental results are compared with the previous data at ambient pressure, and the change in the FS topology and the internal field with pressure is discussed.

## II. EXPERIMENTS

A single crystal of  $\lambda$ -(BETS) $_2$ FeCl $_4$  has triclinic symmetry and has a needlelike shape elongated along the  $c$  axis. The crystallographic  $ac$  plane is the conduction plane, and the  $b$  axis is the least conducting direction. Annealed gold wires of 20  $\mu$ m diameter were directly attached to both of the sample surfaces parallel to the  $ac$  plane with carbon paste; i.e., the current was made to flow along the least-conducting  $b^*$  axis. We use symbols  $a'$  and  $b^*$  for the projections of the  $a$  and  $b$  axes on to the plane perpendicular to the  $c$  axis. (See the figure embedded in Fig. 1.) The defini-

tions of the angles used throughout this paper are also given in Fig. 1. The resistance measurements were performed with a low-frequency lock-in technique. Pressure was generated with a miniature BeCu pressure clamp cell with 8 mm in outer diameter so that it can be rotated in a top-loading dilution refrigerator. A 1:1 mixture of the Daphene 7373 oil and kerosene was used as a pressure medium. Pressure was applied to  $\lambda$ -(BETS) $_2$ FeCl $_4$  at room temperature while the resistance increase of manganin wire gauge was monitored. The maximum pressure of 10.2 kbar was applied, but the pressure after releasing from the press was 8.8 kbar. The sample resistance during pressure application is shown in the lower right inset of Fig. 1. The pressure at low temperature measured from the change of the superconducting transition temperature of high-purity (99.9999%) lead was 6.0 kbar. The transition width was sharp enough for us to ignore the pressure gradient across the sample. The pressure cell was mounted in a rotator and immersed in liquid  $^3$ He or  $^4$ He. The experiments were performed either in 14- and 20-T superconducting magnets at the National Institute for Materials Science (NIMS), Tsukuba, or in a 33 T resistive magnet at the National High Magnetic Field Laboratory (NHMFL), Florida. The azimuthal angle dependence of AMR oscillations was measured with the two-axis rotator probe at Ewha Womans University.

## III. RESULTS

The cooling curves of the resistance under 6 kbar (Fig. 1) show that the AF insulating state is suppressed by applied pressure. Monotonously decreasing metallic resistance is in agreement with the previous report.<sup>11</sup> The kink around 1.3 K indicated by an arrow in Fig. 1 suggests the occurrence of an AF order of the Fe $^{3+}$  spins. A similar behavior is observed in its sister compound  $\kappa$ -(BETS) $_2$ FeBr $_4$ .<sup>14</sup> No sign of superconductivity is found down to 300 mK. The sample pressure cell was kept all through the subsequent experiments. We confirmed the reproducibility of the pressure at low temperature from the AF transition temperature for each experiment. The traces of resistance versus temperature for experiments in the 18-T, 33-T, and 14-T magnets are shown side by side in the main panel of Fig. 1 and show that the temperature of the AF transition around 1.3 K stays the same.

### A. Magnetoresistance

Figures 2(a) and 2(b) represent the field dependence of the interlayer resistance  $R_{b^*}$  under 6 kbar and at 0.3 K for different directions of the magnetic field in the  $a'b^*$  plane. The angle  $\theta$  is measured from the  $b^*$  axis to the magnetic field direction. As the field increases, the antiferromagnetically ordered  $3d$  spins are canted, as evidenced by a slope change indicated by a downward arrow in the inset of Fig. 2(a). The resistance undergoes a bumplike behavior and then gradually increases with further increase of magnetic field. SdH oscillations are clearly visible above 12 T for small  $\theta$ . In the previous report, the bumplike behavior was explained to be an indication of the transition from a canted AF state to a PM state.<sup>15</sup> This behavior is very similar to that of  $\kappa$ -(BETS) $_2$ FeBr $_4$ .<sup>16</sup> The boundary field between the AF and

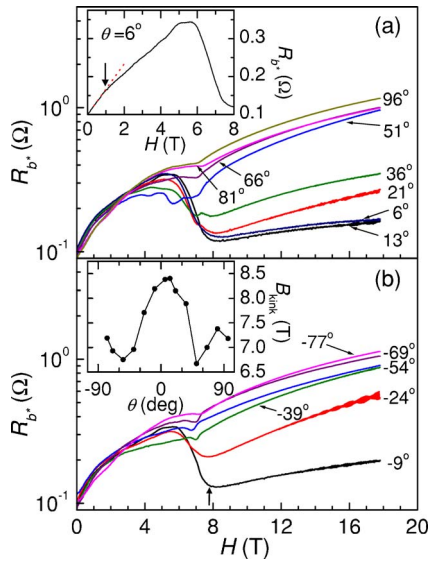


FIG. 2. (Color online) Field-dependent magnetoresistance of  $\lambda$ -(BETS) $_2$ FeCl $_4$  under a pressure of 6 kbar and at a temperature of 0.3 K for different directions of the magnetic field in the  $a^*b^*$  plane. The angle range is positive in (a) and negative in (b). The canted AF transition is indicated in the inset of (a) with downward arrow. Inset of (b) shows angular dependence of  $B_{\text{kink}}$  as defined in the text.

PM states,  $B_{\text{kink}}$ , is identified as a field at the minimum value in magnetoresistance.  $B_{\text{kink}}$  at  $-9^\circ$  is indicated by an upward arrow in the figure. In the inset of Fig. 2(b),  $B_{\text{kink}}$  at various angles shows weaker  $\theta$  dependence than in  $\kappa$ -(BETS) $_2$ FeBr $_4$  by a factor of 2 and has minima around  $\pm 50^\circ$ . This implies that the meaning of the angular dependence of  $B_{\text{kink}}$  in  $\lambda$ -(BETS) $_2$ FeCl $_4$  must be different from that in  $\kappa$ -(BETS) $_2$ FeBr $_4$  for which  $B_{\text{kink}}$  has  $\cos \theta$  dependence and the magnetic easy axis is neatly defined as the in-plane axis ( $c$  axis).<sup>17</sup> In  $\kappa$ -(BETS) $_2$ FeBr $_4$ , the  $\pi$ - $d$  coupling is weak, so only the Fe $^{3+}$  spins are important to the phase boundary between AF and PM states. In case of  $\lambda$ -(BEST) $_2$ FeCl $_4$ , the  $\pi$ - $d$  coupling is much bigger which may cause an asymmetric angle dependence of the  $B_{\text{kink}}$ . Various magnetic property studies of  $\lambda$ -(BETS) $_2$ FeCl $_4$  at ambient pressure have indicated that AF easy axis is near the  $c$  axis. However, Sasaki *et al.* have noted that the magnetic easy axis of  $\lambda$ -(BETS) $_2$ FeCl $_4$  is not directed to any of the crystallographic principal axes.<sup>18</sup> In analogy, we may expect that the magnetic easy axis is the angle of the minimum  $B_{\text{kink}}$ . If only the one of minima  $B_{\text{kink}}$  is an easy axis, it is not far from the easy axis reported by Sasaki *et al.* and strongly against the observation that the easy axis is along the  $c$  axis.

The SdH oscillations of each field scan in Fig. 2 are plotted in Fig. 3(a) as a function of the inverse magnetic field between 14 and 17.8 T. Figure 3(b) shows fast Fourier-transform (FFT) results at  $0^\circ$ . Frequency of  $\alpha$  oscillation which has also been reported at ambient pressure is shifted from  $674 \pm 65$  T to a larger value of 853 T, but the splitting of oscillations is not evident in this limited field range. Two sharp peaks  $\beta_1$  and  $\beta_2$  are newly detected at 4000 and 4276 T. The fact that only the  $\alpha$  orbit is observed at ambient pressure implies that the gap between the closed and open

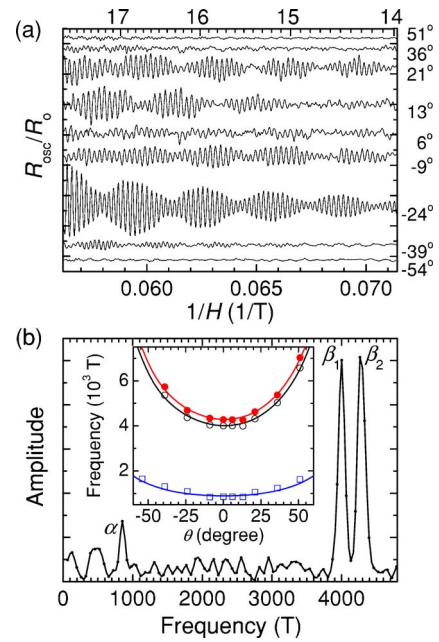


FIG. 3. (Color online) (a) The oscillatory part of the resistance in Fig. 2 with respect to the inverse field between 14 and 17.8 T. The field is also shown in a linear scale on the top axis. (b) FFT result of the SdH oscillation measured at  $0^\circ$ . The inset shows the angular dependences of the FFT frequencies.  $\square$ ,  $\circ$ , and  $\bullet$  symbols represent  $\alpha$ ,  $\beta_1$ , and  $\beta_2$  oscillations, respectively. Solid lines are  $1/\cos \theta$  fittings to each oscillation.

parts of the FS is fairly large. Although there is no information on the band structure under pressure, it can be assumed that no pressure-induced structural transition takes place and that the band structure at high pressure remains essentially the same as that at ambient pressure. The expansion of the FBZ under pressure can be estimated from the increase of the  $\beta$  oscillation frequency because it is assumed to have the same area as the FBZ from the stoichiometry. Unfortunately, any  $\beta$  oscillations have been observed at ambient pressure and we can only estimate the FBZ from the crystal structure at 10 K. The area of the FBZ perpendicular to the  $b^*$  direction corresponds to 4010 T at ambient pressure and at 10 K.<sup>19</sup> The average frequency of the  $\beta$  orbits under pressure of 6 kbar, 4138 T, corresponds to a 1.5% reduction of lattice parameters by pressure. Therefore, we can expect that the closed FS expands faster than the open FS and the gap becomes smaller under pressure. Then it is easier for the electrons to tunnel through the gap, giving rise to a new large magnetic breakdown (MB) orbit. The well-known 2D superconductor  $\kappa$ -(ET) $_2$ Cu(NCS) $_2$  supports our results. In this compound, the pressure of 16.3 kbar increases the area of the closed orbit by 30%, while that of the MB orbit increases only by 6% under the same pressure change.<sup>20</sup> The angular dependence of the SdH frequencies  $\alpha$ ,  $\beta_1$ , and  $\beta_2$  are plotted in the inset of Fig. 3(b). All frequencies are well fitted by  $1/\cos \theta$ , which confirms once more the characteristic 2D nature of magnetoresistance oscillations. The difference between  $\beta$  frequencies follows approximately the inverse cosine behavior and can eventually tell the field direction dependence of  $H_{\text{int}}$  from Eq. (1) if a precise angular depen-



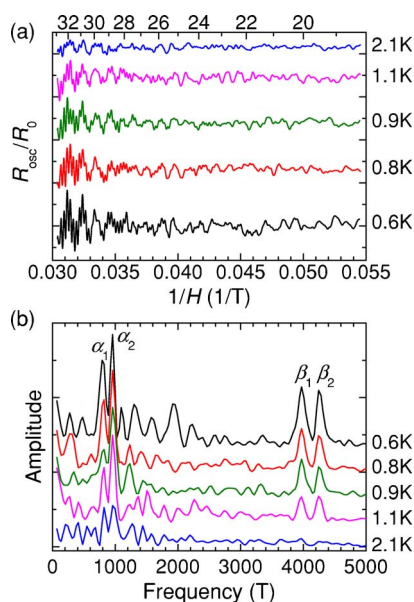


FIG. 4. (Color online) (a) Oscillatory part of the magnetoresistance at 6 kbar and  $\theta=0^\circ$  in the field range from 18 and 33 T at various temperatures. The SdH oscillations survive even until 2.1 K. The top axis shows the field in a linear scale. (b) FFT spectra of the SdH oscillations. The base line at each temperature is vertically shifted for clarity.

dence of  $m_{\text{eff}}$  is determined. We also note an oscillatory behavior in the magnetoresistance below  $B_{\text{kink}}$ , which becomes more evident at higher angles (Fig. 2). It is reminiscent of SdH oscillations arising from small closed orbits, because the FS is reconstructed by the AF order below  $B_{\text{kink}}$ . However, no distinct peak is found in the FFT spectra. The number of the observed waves may not be large enough to make a distinct peak.

To clarify the presence of the splitting in the  $\alpha$  oscillation, SdH oscillations are measured up to 33 T at several temperature values. The magnetic field is applied along the  $b^*$  axis—i.e.,  $\theta=0$ . Figure 4(a) shows the oscillatory amplitude of the magnetoresistance as a function of inverse magnetic field at several temperature values after the slowly varying background is subtracted. The oscillatory behavior can be observed at least up to 2.1 K. The FFT spectra of the SdH oscillations in the field range between 18 and 33 T are displayed in Fig. 4(b). Base lines are shifted equally to increase readability. The splitting of  $\alpha$  oscillation is observed and the amplitudes of the FFT result in  $\alpha$  oscillations are pronounced better than that in  $\beta$  oscillation.  $\alpha_1$ ,  $\alpha_2$ ,  $\beta_1$ , and  $\beta_2$  have values of 803, 957, 3973, and 4255 T, which are in fair agreement with the values obtained at low magnetic field.

The amplitude of oscillations divided by the temperature as a function of temperature, the so-called mass plot, is presented in Fig. 5. Circle and diamond symbols represent  $\alpha$  and  $\beta$  oscillations, respectively, and solid lines are fits to the LK formula. In the 2.1-K data of the  $\beta$  orbit it is hard to discern the peak position. Plotting  $\alpha_1$ ,  $\alpha_2$ ,  $\beta_1$ , and  $\beta_2$  orbits individually, the effective masses of those orbits are obtained as  $(3.2\pm 0.6)m_0$ ,  $(2.6\pm 0.2)m_0$ ,  $(5.2\pm 0.1)m_0$ , and  $(5.8\pm 0.5)m_0$ , respectively, where  $m_0$  is the free electron mass.

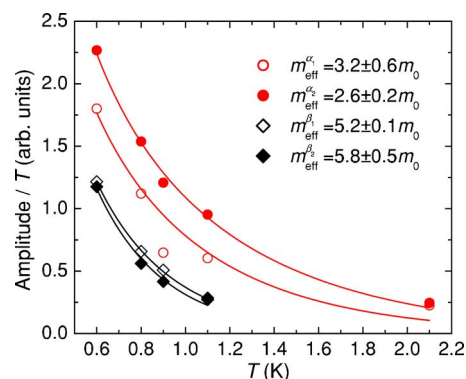


FIG. 5. (Color online) Temperature dependence of the amplitudes of  $\alpha_1$ ,  $\alpha_2$ ,  $\beta_1$ , and  $\beta_2$  oscillations divided by temperature are represented with  $\circ$ ,  $\bullet$ ,  $\diamond$ , and  $\blacklozenge$  symbols, respectively. Solid lines are the LK fittings to them.

The average values are  $(2.9\pm 0.3)m_0$  in  $\alpha$  and  $(5.5\pm 0.3)m_0$  in  $\beta$  orbit. For the closed-orbit oscillations, the effective mass falls from  $4.1m_0$  at the ambient pressure to  $2.9m_0$  under 6 kbar. As for the MB orbit, the effective mass of  $5.5m_0$  is lighter than that in other BETS compounds containing magnetic ions. Hydrostatic pressure will bring the BETS molecules closer together and hence broaden the energy band. So the decrease in effective mass with pressure is strongly related to the suppression of interaction between  $\pi$  electrons which depends critically on the bandwidth. As stated earlier, the internal field  $H_{\text{int}}$  can be directly calculated from the difference of frequencies,  $2\Delta F$ . Applying the expression of Eq. (1) for  $H_{\text{int}}$  to the  $\alpha$  and  $\beta$  orbits,  $\Delta F_\alpha=77$  T and  $\Delta F_\beta=141$  T give the estimated values for  $H_{\text{int}}^\alpha=53$  T and  $H_{\text{int}}^\beta=51$  T, assuming that the  $g$  factor is 2. The  $g$  factor in molecular conductors is close to the free electron value of 2.0023. The deviation from 2 comes from the second-order perturbation of the spin-orbit interaction, so it is generally small. In case of  $\lambda$ -(BETS) $_2$ FeCl $_4$ , the molecular orbitals are widely spread, so the spin-orbit interaction is much smaller than that of atomic  $\pi$  electrons. Therefore, the assumption of  $g=2$  under pressure is quite reasonable.

According to the Jaccarino-Peter effect,  $H_{\text{int}}$  is mainly determined by  $\pi$ - $d$  interactions.<sup>5</sup> The strong increase of the  $H_{\text{int}}$  up to 52 T in average under 6 kbar may simply be understood with the increased  $\pi$ - $d$  interaction under pressure. There have been some results inconsistent with ours. The susceptibility measurements under various pressures, performed by Sato *et al.*, suggested that pressure weakens the  $\pi$ - $d$  coupling and only  $d$ -spin systems tend to be antiferromagnetically ordered.<sup>21</sup> It is expected that reducing the exchange interaction will produce a lower internal field. Under a very small pressure about 1.4 kbar in  $\lambda$ -(BETS) $_2$ FeCl $_4$ , the FISC state becomes broad.<sup>13</sup> However, Mori and Katsuhara estimated magnetic interactions for  $\lambda$ -(BETS) $_2$ FeCl $_4$  on the basis of the extended Hückel-type calculation.<sup>22</sup> In the simple mean-field approximation, the AF ordering temperature  $T_N$  is determined both by the direct  $d$ - $d$  interaction and by the indirect  $\pi$ - $d$  interaction. The contribution of the  $d$ - $d$  and  $\pi$ - $d$  interactions to  $T_N$  at ambient pressure is 3.73 K and 2.49 K, respectively. Even though the  $\pi$ - $d$  interaction in-

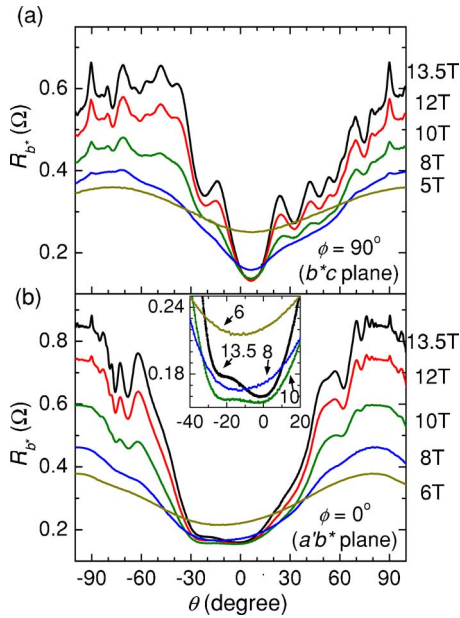


FIG. 6. (Color online) Angular-dependent magnetoresistance oscillations for different magnetic fields under a pressure of 6 kbar and at a temperature of 1.7 K. The magnetic field is rotated in the  $b^*c$  plane (a) and the  $a'b^*$  plane (b), respectively. The resistance dip around  $0^\circ$  at  $\phi=0^\circ$  is enlarged in the inset of (b).

creases under 6 kbar,  $T_N$  can be decreased by means of the weakened  $d-d$  interaction. According to Ref. 21, the AF ordering temperature of  $\text{Fe}^{3+}$  spins, determined by the peak temperature of susceptibility, is decreased by applying pressure and that can support the decrease of the  $d-d$  interaction under pressure. At present, the detailed mechanism of the pressure effect on the interaction between  $\text{Fe}^{3+}$  spins and conduction electrons is not clear.

### B. Angular-dependent magnetoresistance

For a simply corrugated cylindrical FS, the angular position  $\theta_N$  of the AMR peak satisfies  $|\tan \theta_N| = \pi/dk_{\parallel}(N-1/4)$ , where  $N$  is an integer,  $d$  the interlayer distance, and  $k_{\parallel}$  the maximum Fermi wave-vector projection on the plane of rotation of the field. The slope of a plot of  $\tan \theta_N$  against  $N$  may thus be used to find one of the dimensions of the FS.<sup>23,24</sup> Figure 6 presents the AMR oscillations at 6 kbar and 1.7 K under various magnetic field strengths up to 13.5 T for two different azimuthal angles:  $\phi=90^\circ$  (a) and  $0^\circ$  (b). The orientation of the magnetic field rotates in the  $b^*c$  and  $a'b^*$  planes, respectively. Distinctive peak patterns are present, and their angular positions are independent of the magnetic field strength. The coherence peaks can be readily discerned from the raw data when the magnetic field lies close to the  $ac$  plane. The overall peak patterns are also better resolved under pressure than at ambient pressure.<sup>6</sup> The peak positions of the AMR oscillations are quantitatively explained in terms of Yamaji's model. The AMR oscillations at  $\phi=0^\circ$  and  $90^\circ$  have periods  $\Delta \tan \theta_N$  of 1.29 and 0.45, respectively. The lengths of the Fermi wave vectors are then calculated to be 0.13 and 0.38 Å. A detailed analysis of the AMR oscillations is given later.

Although the observed AMR oscillations can be understood in terms of the conventional Yamaji resonances, there are some points we need to mention. First, the AMR oscillations are very asymmetric between positive and negative angles. In Fig. 6(a), the resistance dip is evident around  $6^\circ$  instead of  $0^\circ$  in the  $b^*c$ -plane rotation. The asymmetry reflects the triclinic lattice structure of the title compound with asymmetric corrugation of the FS along the  $k_b$  direction. Second, the AMR shows anomalous behavior around  $\theta=0^\circ$  in the  $a'b^*$ -plane rotation. As shown in the inset of Fig. 6(b), a dip is seen around  $\theta=-10^\circ$  below 8 T, but it splits into two broad dips above 10 T, the positions of which do not correspond to any crystallographic direction. Third, the first peaks observed around  $\pm 60^\circ$  in the  $a'b^*$  rotation are assigned to  $N=\pm 2$  peaks considering the phase term of the Yamaji condition. A possible interpretation is that for small values of  $\theta$ , and hence for a large perpendicular magnetic field to the conducting plane, two splitting FS's by the internal field may correlate to vanish the Yamaji resonance.

The measurements of the AMR oscillations at various azimuthal angles  $\phi$  were also performed. In Fig. 7(a), the angular positions of the peaks in  $\tan \theta_N$  are plotted in the polar coordinates of  $\phi$ . It can be found that the oscillations consist of three different series, which are plotted by solid circles, solid triangles, and solid squares. Figure 7(b) shows a polar plot of  $k_{\parallel}$  derived from the periodicity of the AMR oscillations in (a). Note that one set of AMR oscillations (solid circles) has a period  $\Delta(\tan \theta_N)$  of between 0.42 and 0.66, depending on the azimuthal angle  $\phi$ . Assuming that the AMR oscillations arise from a closed orbit, we obtain a 2D FS shown by a bold solid ellipse. This area corresponds to about 100.7% of the FBZ—i.e., that of the MB orbit. On the other hand, the AMR oscillations which are plotted by the solid triangles have a larger period in  $\Delta(\tan \theta_N)$  between 0.74 and 3.12, giving a 2D FS indicated by a thin solid ellipse (about 16% of the FBZ), which can be ascribed to the closed orbit. These data seem roughly consistent with the calculated band structure [Fig. 7(c)]. Concerning the oscillations with the largest period in  $\Delta(\tan \theta_N)$  plotted by closed squares, it can be regarded as a very small 2D FS [dotted line in (b)], which has not been observed in the SdH oscillation measurements. A possible scenario is that the original 1D FS is elongated in the  $k_c$  direction under the high pressure and cut across the zone boundary. In such a case, we may observe a small closed orbit near the zone boundary, causing AMR oscillations with a long period  $\Delta(\tan \theta_N)$ .

When the magnetic field lies almost parallel to the conducting plane, a peak in resistance is readily observed. The widths of the narrow peak at various azimuthal angles  $\phi$  are shown in Fig. 8. For  $\kappa\text{-(ET)}_2\text{Cu(NCS)}_2$  with similar FS topology, the peak width under in-plane field was analyzed in detail.<sup>25</sup> Such peaks generally arise from small closed orbit of the sides of both the 1D and 2D FS's, although the peaks were originally ascribed to the closed orbit on the 2D FS only.<sup>26</sup> When 1D and 2D FS's coexist, the peak width show very complicated angular dependence. For this material, the ambiguity of the FS structure does not allow us to analyze the data in detail. However, it is very likely that the complicated behavior in Fig. 8 has a similar origin as discussed in  $\kappa\text{-(ET)}_2\text{Cu(NCS)}_2$ .

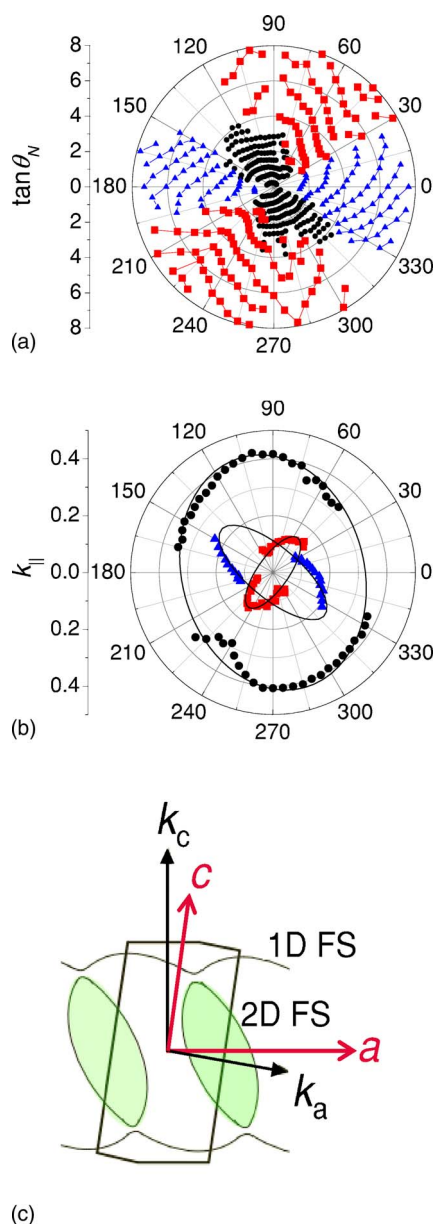


FIG. 7. (Color online) (a) Positions of the resistance peaks in the AMR plotted in the polar coordinates of  $\tan \theta$  versus  $\phi$ . (b) Polar plot of the wave vector  $k_{\parallel}$  for three series of AMR's. (c) FS of  $\lambda$ -(BETS)<sub>2</sub>FeCl<sub>4</sub> obtained from the band structure calculation (Ref. 1).

#### IV. SUMMARY

The variety of electronic phase transitions in  $\lambda$ -(BETS)<sub>2</sub>FeCl<sub>4</sub> under magnetic field apparently originates from the interaction between Fe<sup>3+</sup> *d* electrons and  $\pi$  conduction electrons on the BETS molecules. Applying pressure is expected to change the intervals between molecules and to affect  $\pi$  and *d* spin interactions. The observation of SdH and AMR oscillations of  $\lambda$ -(BETS)<sub>2</sub>FeCl<sub>4</sub> under pressure has allowed us to study the effect of pressure on the FS, effective

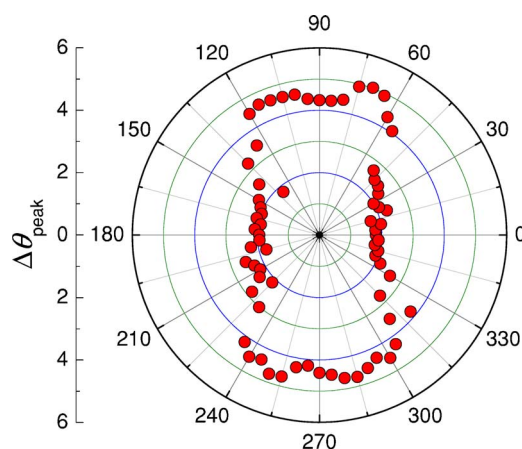


FIG. 8. (Color online) Polar plot of the width of the peak structure around  $\theta=90^\circ$ .

mass and the internal field. The temperature dependence of  $\lambda$ -(BETS)<sub>2</sub>FeCl<sub>4</sub> at 6 kbar shows that the AF insulating state is suppressed. As the magnetic field is applied perpendicular to the conduction plane, a phase transition from a canted AF to a PM state takes place, and then SdH oscillations occur. FFT spectra of the SdH oscillations give two distinct frequency peaks  $\alpha$  and  $\beta$ , both having a splitting in frequency. Compared with the results at ambient pressure, the frequencies of the  $\alpha$  oscillations are shifted to larger values and two new high-frequency peaks can be attributed to the magnetic breakdown orbit across the smaller gap between the closed and open FS's. The decreased effective mass is ascribed to the suppression of the correlation between the conduction electrons due to enhancement of the bandwidth. The internal field determined from the splitting of FFT frequency increases from 32 T to about 52 T under a pressure of 6 kbar. The angular dependence of the transition field from the canted AF to paramagnetic state exhibits the fact that the magnetic easy axis is tilted from the crystallographic axes. The AMR oscillations suggest the existence of a small closed orbit under high pressure which has not been observed in the SdH oscillations.

#### ACKNOWLEDGMENTS

This work was supported by Korea Science and Engineering Foundation Grants Nos. R01-2003-000-10470-0(2005) and F01-2001-000-20007-0 and by Korea Research Foundation Grant No. R14-2003-027-01000-0. Y.J.J. acknowledges the support from the 10th Winter Institute Program of KOSEF-JSPS for her stay at NIMS. S.U. and T.T. acknowledge support from a Grant-in-Aid for Scientific Research from the Ministry of Education, Culture, Sports, Science and Technology (No. 15073225) and from the Japan Society for the Promotion of Science for Young Scientists. A part of this work was performed at NHMFL, which is supported by National Science Foundation Cooperative Agreement No. DMR-0084173 and by the State of Florida.



- \*Current address: National High Magnetic Field Laboratory, Florida State University, Tallahassee, Florida 32310, USA.
- †Current address: Materials Science and Technology Division, Korea Institute of Science and Technology, Seoul 136-791, Korea.
- ‡Author to whom correspondence should be addressed. Electronic address: wkang@ewha.ac.kr
- <sup>1</sup>H. Kobayashi, H. Tomita, T. Naito, A. Kobayashi, F. Sakai, T. Watanabe, and P. Cassoux, *J. Am. Chem. Soc.* **118**, 368 (1996).
  - <sup>2</sup>L. Brossard *et al.*, *Eur. Phys. J. B* **1**, 439 (1998).
  - <sup>3</sup>L. Balicas, J. S. Brooks, K. Storr, S. Uji, M. Tokumoto, H. Tanaka, H. Kobayashi, A. Kobayashi, V. Barzykin, and L. P. Gor'kov, *Phys. Rev. Lett.* **87**, 067002 (2001).
  - <sup>4</sup>S. Uji, H. Shinagawa, C. Terakura, T. Terashima, T. Yakabe, Y. Terai, M. Tokumoto, A. Kobayashi, H. Tanaka, and H. Kobayashi, *Nature (London)* **410**, 908 (2001).
  - <sup>5</sup>V. Jaccarino and M. Peter, *Phys. Rev. Lett.* **9**, 290 (1962).
  - <sup>6</sup>S. Uji, H. Shinagawa, C. Terakura, T. Terashima, T. Yakabe, Y. Terai, M. Tokumoto, A. Kobayashi, H. Tanaka, and H. Kobayashi, *Phys. Rev. B* **64**, 024531 (2001).
  - <sup>7</sup>D. Shoenberg, *Magnetic Oscillations in Metals* (Cambridge University Press, Cambridge, England, 1984).
  - <sup>8</sup>O. Cépas, R. H. McKenzie, and J. Merino, *Phys. Rev. B* **65**, 100502(R) (2002).
  - <sup>9</sup>S. Uji, C. Terakura, T. Terashima, T. Yakabe, Y. Terai, M. Tokumoto, A. Kobayashi, F. Sakai, H. Tanaka, and H. Kobayashi, *Phys. Rev. B* **65**, 113101 (2002).
  - <sup>10</sup>A. Sato, E. Ojima, H. Kobayashi, Y. Hosokoshi, K. Inoue, A. Kobayashi, and P. Cassoux, *Adv. Mater. (Weinheim, Ger.)* **11**, 1192 (1999).
  - <sup>11</sup>H. Tanaka, T. Adachi, E. Ojima, H. Fujiwara, K. Kato, H. Kobayashi, A. Kobayashi, and P. Cassoux, *J. Am. Chem. Soc.* **121**, 11243 (1999).
  - <sup>12</sup>H. Akutsu, K. Kato, E. Arai, H. Kobayashi, A. Kobayashi, M. Tokumoto, L. Brossard, and P. Cassoux, *Solid State Commun.* **105**, 485 (1998).
  - <sup>13</sup>L. Balicas, V. Barzykin, K. Storr, J. S. Brooks, M. Tokumoto, S. Uji, H. Tanaka, H. Kobayashi, and A. Kobayashi, *Phys. Rev. B* **70**, 092508 (2004).
  - <sup>14</sup>E. Ojima, H. Fujiwara, K. Kato, and H. Kobayashi, *J. Am. Chem. Soc.* **121**, 5581 (1999).
  - <sup>15</sup>Y. J. Jo, H. Kang, T. Tanaka, M. Tokumoto, A. Kobayashi, H. Kobayashi, S. Uji, and W. Kang, *J. Phys. IV* **114**, 323 (2004).
  - <sup>16</sup>T. Konoike, S. Uji, T. Terashima, M. Nishimura, S. Yasuzuka, K. Enomoto, H. Fujiwara, B. Zhang, E. Fujiwara, and H. Kobayashi, *Phys. Rev. B* **72**, 094517 (2005).
  - <sup>17</sup>L. Balicas *et al.*, *Solid State Commun.* **116**, 557 (2000).
  - <sup>18</sup>T. Sasaki, H. Uozaki, S. Endo, and N. Toyota, *Synth. Met.* **120**, 759 (2001).
  - <sup>19</sup>According to measurement of the SdH oscillations at ambient pressure, two  $\alpha$  oscillation frequencies, 609 and 737 T, correspond to 14% and 17% of the FBZ, respectively. Then, the estimated FBZ is 4340 T, which is pretty much larger than our calculation of the FBZ at 6 kbar. We doubt the area of the FBZ at ambient pressure is calculated from the lattice parameters at room temperature in Ref. 6.
  - <sup>20</sup>J. Caulfield, W. Lubczynski, F. L. Pratt, J. Singleton, D. Y. K. Ko, W. Hayes, M. Kurmoo, and P. Day, *J. Phys.: Condens. Matter* **6**, 2911 (1994).
  - <sup>21</sup>A. Sato, E. Ojima, H. Akutsu, H. Kobayashi, A. Kobayashi, and P. Cassoux, *Chem. Lett.* **1998**, 673 (1998).
  - <sup>22</sup>T. Mori and M. Katsuhara, *J. Phys. Soc. Jpn.* **71**, 826 (2002).
  - <sup>23</sup>K. Yamaji, *J. Phys. Soc. Jpn.* **58**, 1520 (1989).
  - <sup>24</sup>M. V. Kartsovnik, V. N. Laukhin, S. I. Pesotskii, I. F. Schegolev, and V. M. Yakovenko, *J. Phys. I* **2**, 89 (1992).
  - <sup>25</sup>P. A. Goddard, S. J. Blundell, J. Singleton, R. D. McDonald, A. Ardavan, A. Narduzzo, J. A. Schlueter, A. M. Kini, and T. Sasaki, *Phys. Rev. B* **69**, 174509 (2004).
  - <sup>26</sup>N. Hanasaki, S. Kagoshima, T. Hasegawa, T. Osada, and N. Miura, *Phys. Rev. B* **57**, 1336 (1998).